International Journal of Thermophysics, Vol. 28, No. 1, February 2007 (© 2007)
DOI: 10.1007/s10765-007-0167-1

GERG Project: Development and Setup of a New Combustion Reference Calorimeter for Natural Gases

M. Jaeschke,[1,2] A. Schmücker,[1] A. Pramann,[3] and P. Ulbig[3]

Received May 23, 2006

Natural gas plays an important role for worldwide energy supply. For billing purposes precise metering of volume and superior calorific value are very important. At present, only a few institutions worldwide are able to determine the superior calorific value (SCV) of gases and their mixtures with an uncertainty of less than 0.2%. Calculations of SCV's of natural gases using the data of ISO 6976 provides a similar uncertainty as experimental approaches. For this reason a GERG (Groupe Européen de Recherches Gazières) project was initiated to develop a new reference calorimeter for determining the SCV of flammable gases (natural gases), based on the principle of Rossini for a combustion calorimeter. The purpose of such a reference calorimeter is to determine the SCV of pure gases and gas mixtures with an uncertainty of less than 0.05%. The overall uncertainty budget for the SCV is mainly influenced by the mass determination and temperature measurement. An automated weighing and calibration device is used to measure the mass of the combusted gas with an experimental uncertainty of approx. 0.015%. In addition to the experiment, the flow and temperature field in the calorimeter were simulated. These simulations help to reduce each of the combined uncertainties for the combustion and calibration experiment resulting from the temperature measurement. The determination of the adiabatic temperature rise is performed analytically. The assumptions made by early investigators were carefully reconsidered for the first time. The analysis of the temperature–time curves considers (a) the method of evaluation, (b) the interval length of the main period, (c) the location of the heat release during the calibration experiment, and (d) the temperature sensor location.

KEY WORDS: adiabatic temperature rise; calorific value; energy; isoperibolic combustion calorimeter; natural gas; traceability; uncertainty

[1]E.ON Ruhrgas AG, Halterner Straße 125, D-46284 Dorsten, Germany.
[2]To whom correspondence should be addressed. E-mail: m-m-jaeschke@gmx.de
[3]Physikalisch-Technische Bundesanstalt, Bundesallee 100, D-38116 Braunschweig, Germany.

1. INTRODUCTION

Energy measurement is one of the central tasks in the gas industry. Compared with the measurement and billing of electrical energy, determining the energy contained in a gas involves a much greater effort and is far more complex because fluid mechanics and the thermodynamic and calorific properties of natural gases have to be taken into account.

A brief overview is given of existing methods to measure the calorific value in the gas industry. Improved standards for verification are necessary to reduce the uncertainty in calorific value measurements and the uncertainty in calorific reference data. For this purpose the project to develop an improved reference calorimeter was launched.

In a feasibility study the possibility of reliably verifying results of direct or indirect measurements of the calorific value by way of a traceability chain was discussed and the possibilities of developing a reference calorimeter [1] was investigated. As a result, six partners finally agreed to develop an isoperibolic combustion calorimeter based on the principle of a Rossini combustion calorimeter [2,3]. The concept for such a reference calorimeter has been developed by PTB and cross-checked by the members participating in the project. The main module of the mass determination system as well as the module of the burner system immersed in a calorimeter with a constant jacket temperature was designed and has been tested.

The assumptions in determining the adiabatic temperature rise from the temperature measurement during the experiment and the calibration which contribute mainly to the total uncertainty budget of the calorimeter have been analyzed. A simulation of the flow and temperature field in the burner helped to characterize these contributions.

1.1. Calorific Value Determination

At large gas receiving or delivery stations, the superior calorific value, H_S, is either measured with a calorimeter or determined by compositional analysis using a process chromatograph [4,5]. The calorific value is measured together with the metered volume. In other cases a constant gas quality and, therefore, calorific value is assigned to a certain regional district with several delivery stations and measured only once. The uncertainty of the calorific value measured under field conditions is between 0.3% and 0.5%. Other field instruments may use indirect combustion methods [5,6] or inferential/correlative methods with further increased uncertainty [5,7,8].

The uncertainty of calorific values determined with field instruments or calculated from compositional analysis has only marginally improved

over the past decades. The reason for this is that all these instruments or measuring devices need to be calibrated. Primary standards or primary reference materials used to realize a traceability chain achieves at present, an uncertainty of about 0.2%. Even the calorific value of pure components proposed in ISO 6976 [4] derived from measurements made in the 1930s and 1970s have an uncertainty of at least 0.1% (2k). Moreover, the "uncertainty" given, e.g., of methane, reflects only the repeatability of the measurements. Possible systematic errors of measurements conducted in the past cannot be traced back.

A traceable reference calorimeter will improve the situation and reduce thereby the risk associated with high uncertainty in field energy measurement. Depending on the long-term stability and repeatability of field instruments, an uncertainty of 0.15–0.3% can be achieved.

2. DEVELOPMENT OF A COMBUSTION REFERENCE CALORIMETER

2.1. Scope

A GERG working group was set-up in 2002 to develop the new combustion reference calorimeter on the basis of the Rossini principle. The working range of the new calorimeter was set for calorific values of 42–56 $kJ \cdot g^{-1}$ on a mass basis or approximately 32–48 $MJ \cdot m^{-3}$ on a volumetric basis (the metered volume may be taken at 273.15 K and 101.325 kPa). The calorimeter was designed for natural gases (mixtures of hydrocarbons, inert gases, nitrogen (up to 15%) and carbon dioxide (up to 10%)), and for synthetic natural gases as well as for pure gases (methane, ethane, propane, and butane). The calorific value may be given for a reference temperature of 298.15 K for the combustion process.

The project is divided into two parts. Part 1 deals with the development of a reference calorimeter. In Part 2 the uncertainty of less than 0.05% at a confidence level of 95% ($k = 2$) is demonstrated for the calorimeter.

E.On Ruhrgas will apply for the reference calorimeter to be accredited by the Deutscher Kalibrierdienst (DKD, German Calibration Service). An international comparison involving other high-accuracy calorimeters developed at the Physikalisch-Technische Bundesanstalt (PTB, Germany) and the Laboratoire National D'Essais (LNE, France) is planned and will enhance and support international acceptance for the new GERG reference calorimeter.

2.2. Concept of the New Combustion Reference Calorimeter

In a feasibility study Advantica Technologies (United Kingdom), PTB (Germany), E.On Ruhrgas AG (Germany), and Snam Rete Gas (Italy) investigated the possibilities of developing a reference calorimeter. The feasibility study suggested that an uncertainty of 0.05% can be achieved for the Rossini type combustion calorimeter [1]. The study suggested improvements and refinements to former calorimeters operating on the Rossini principle (see Table I). Figure 1 shows the components needed for the periphery of the calorimeter.

The gas is supplied to a balance to weigh the amount of gas used for combustion, which approximates the mass of the burnt gas, m_{gas}. To avoid buoyancy corrections to the weighing result, this balance is placed in a vacuum chamber, which may be evacuated to a pressure of less than 1 mbar. A calibration robot allows weighing results to within an uncertainty of 0.015% and traceability back to the international standard of

Table I. Comparison of Main Components of Apparatus with Previous Investigations

	Rossini [2]	Pittam and Pilcher [3]	OFGEM[11]	GERG project (solution examined)
Mass determination	– produced water	– produced CO_2	– weighing by difference	– weighing by difference (automatically)
Gas analysis	– CO_2 absorption tubes	– water absorption tubes	– CO - analyzer water absorption tubes	– CO-, C_nH_m-, NO analyzer – water absorption tubes
Temperature measurement	– standard platinum resistance thermometer	– standard platinum resistance thermometer	– standard platinum resistance thermometer	– thermistor – standard platinum resistance thermometer
Calibration	– electrical (heating tube)	– burning hydrogen and oxygen	– electrical (heating tube)	– electrical (heating wire wound around the burner)
Operating conditions	– isoperibolic	– isoperibolic	– isoperibolic	– isoperibolic

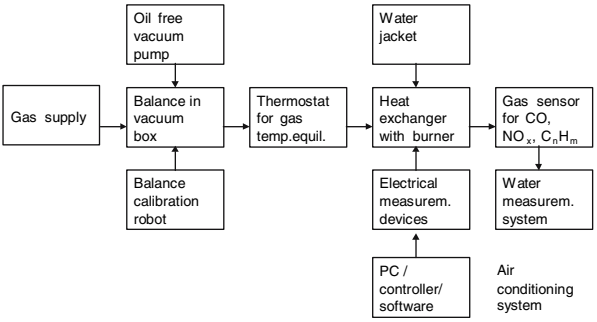

Fig. 1. Planned Rossini calorimeter including periphery.

mass as has been explained in detail in Refs. 9 and 10. The gas is fed to the burner, which is placed in a calorimeter. The heat of combustion, H_s, causes a temperature increase, $\Delta T_{ad,comb}$, in the calorimeter. Multiplying this temperature rise by the heat capacity, $C_{cal,comb}$, of the calorimeter, gives the amount of energy released. K is the energy correction value explained in a later section.

$$\frac{m_{gas}H_s - K}{E_{elec}} = \frac{C_{cal,comb}\Delta T_{ad,comb}}{C_{cal,elec}\Delta T_{ad,elec}} \tag{1}$$

The calorimeter is operated as a *heat comparator*. Measured temperatures are the indicators of the heat comparator, and the corresponding calculated adiabatic temperature rises ΔT_{ad} are the measures for this kind of instrument. This means that the amount of heat released in the combustion experiment is about the same as the heat released during electrical calibration. The quantitative expression of the equality of both processes is given by the ratio of the adiabatic temperature rises, ΔT_{ad}, for both processes. The heat capacity of the calorimeter is determined from an electrical calibration, where the electrical energy, E_{elec}, leads to the same temperature increase, $\Delta T_{ad,elec}$, as in the combustion experiment. In this case it is assumed that $C_{cal,elec}$ and $C_{cal,comb}$ are about equal.

The method used to calculate the adiabatic temperature rise in the calorimeter during combustion or calibration will be discussed in detail later. The uncertainty of the temperature rise for these two experiments contributes essentially to the overall uncertainty of the calorimeter.

Other corrections to compensate for imperfect processes have only minor effects on the overall uncertainty, such as side reactions coupled to the combustion of gases, which produces residual hydrocarbons, carbon monoxide, nitrogen oxides, and fractions of water leaving as vapor or condensing as liquid in the calorimeter. Water leaving the calorimeter as vapor

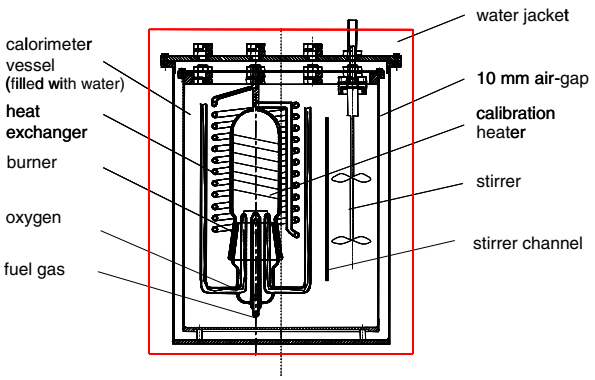

Fig. 2. Schematic diagram of the calorimeter.

results in an energy loss, water condensing inside the calorimeter changes its heat capacity. Although of minor importance, they are accounted for in the evaluation of the experimental results.

2.3. Design of Calorimeter and Burner

The combustion of the sample gas takes place inside the burner. The heat of combustion is transferred from the burner assembly to the heat exchange fluid (water) with which the calorimeter vessel is filled (see Fig. 2). The calorimeter vessel is surrounded by a 10-mm wide air gap and then by a thermostatic water jacket. To minimize heat transfer due to radiation between the calorimeter vessel and the thermostatic water jacket, the surfaces are electrolytically polished. The sample gas, oxygen, and argon are supplied to the burner. Argon does not participate in the reaction, but it serves to stabilize the flame and improve the combustion properties of the fuel gas [11]. The flame thus is lifted, and deposits at the burner tip are avoided [12]. A 50-Ω heater was designed as a winding wire around the calorimeter burner for electrical calibration. This arrangement in the immediate vicinity of the burner closely approximates the energy source during the combustion experiment. The effect of slight differences in the two heat sources on the temperature rise and field in the calorimeter will be discussed later.

3. THEORY OF THE ADIABATIC TEMPERATURE RISE

The adiabatic temperature rise is the temperature increase in the calorimeter under the condition that the heat of combustion is completely

released and stored in the calorimeter, i.e., the calorimeter has an adiabatic wall which prevents any heat exchange with the surroundings. The adiabatic temperature rise is used to determine the heat capacity of the calorimeter by electrical calibration as well. The temperature rise by the combustion and the calibration experiment determines the calorific value (see Eq. (1)). Therefore, most attention is focused on measuring these quantities.

3.1. Temperature Rise in an Adiabatic Calorimeter

To establish an adiabatic wall, the jacket temperature would need to be heated to the actual temperature of the calorimeter. Thus, heat flowing between the calorimeter and its surroundings would be negligible. The temperature increase, ΔT_{ad}, would be directly determined by measuring the initial temperature in the calorimeter bath at the beginning of the experiment, T_{mi}, when the gas is ignited, and the final temperature, T_{mf}, at its end.

$$\Delta T_{ad} = T_{mf} - T_{mi} \tag{2}$$

By measuring the temperature difference between the jacket and calorimeter, the adiabatic jacket/wall may in principle be controlled. Therefore, a sensor with a short response time would be necessary. For a reference calorimeter the temperature difference would need always to be $\ll 0.5\,\mathrm{mK}$ which is extremely difficult to realize. The temperature rise in a calorimeter with adiabatic surroundings could then be measured with a standard platinum resistance thermometer attached to a resistance bridge with high resolution and accuracy.

3.2. Adiabatic Temperature Rise in an Isoperibolic Calorimeter

A strictly adiabatic calorimeter in this application is evidently impractical. Instead we have chosen to operate the calorimeter in an isoperibolic configuration, i.e., a calorimeter with an isoperibolic jacket. The temperature rise in such a calorimeter is measured with a standard platinum resistance thermometer attached to a resistance bridge with high resolution and accuracy or a thermistor with fast response. In this case the calculation of the adiabatic temperature rise must be corrected for the energy exchanged with the surroundings. The following equation gives the energy balance for the experiment:

$$m_{cal} c_{p,cal} \frac{dT_{cal}}{dt} = \dot{Q}_{prod} + \dot{Q}_{cond} + \dot{Q}_{conv} + \dot{Q}_{rad} + \dot{Q}_{gas} + \dot{Q}_{stir} + \dot{Q}_{ign} \tag{3}$$

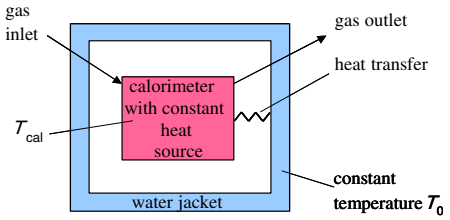

Fig. 3. Two-body model of an isoperibolic calorimeter.

where

m_{cal} is the mass of the calorimeter,

$c_{p,cal}$ is the specific heat capacity of the calorimeter,

T_{cal} is the temperature of the calorimeter (volume averaged),

$\dot{Q}_{prod}$ is the heat flux due to production (combustion, electrical heating) within the calorimeter,

$\dot{Q}_{cond}$ is the heat flux due to conduction between the calorimeter and water jacket,

$\dot{Q}_{conv}$ is the heat flux due to convection (air gap between calorimeter and water jacket),

$\dot{Q}_{rad}$ is the heat flux due to radiation,

$\dot{Q}_{gas}$ is the heat flux due to enthalpy differences of inlet and outlet gases,

$\dot{Q}_{stir}$ is the heat flux due to production (stirrer) within the calorimeter, and

$\dot{Q}_{ign}$ is the heat flux due to production (ignition) within the calorimeter.

Using an isoperibolic calorimeter, the adiabatic temperature increase may be determined by the Regnault–Pfaundler method [13]. The method is based on the assumption of a two-body model of a calorimeter (Fig. 3). The two bodies are the inner calorimeter and the water jacket. Both bodies are connected via heat transfer processes of conduction, convection, and radiation. The outer water jacket remains at a constant temperature, T_0.

For small temperature differences the heat transfer of the calorimeter with its surroundings, following, e.g., the combustion experiment, may be given by the relation:

$$\dot{Q}_{\text{heat transfer}} = \kappa (T_0 - T_{cal}(t)) \tag{4}$$

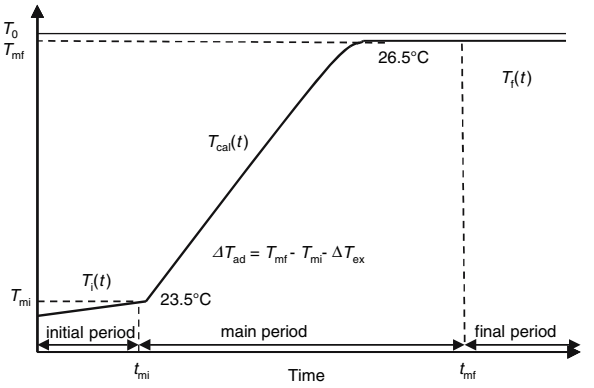

Fig. 4. Determination of the adiabatic temperature rise.

where

κ is the heat transfer coefficient for the calorimeter with surroundings,

T_0 is the temperature of the water jacket, and

T_{cal} is the temperature of the calorimeter (surface averaged).

In this case all heat transfer mechanisms are considered to show linear behavior and can be described with the heat transfer coefficient, κ. Thermal isolation in the air gap reduces heat flux by conduction and convection. Conducting the gas pipes through a thermostat minimizes heat flux due to enthalpy differences.

4. DETERMINATION OF THE ADIABATIC TEMPERATURE RISE

Usually an experiment starts at a temperature inside the calorimeter below T_0. Due to the heat transfer between both bodies, the temperature of the calorimeter increases slightly. This period is called the *initial period*. After some minutes the combustion starts and this leads to a high-temperature increase during the so-called *main period*. After the burner is switched-off, the temperature of the calorimeter increases further slightly due to heat transfer. After the heat is completely released and distributed, the *final period* starts. A schematic temperature–time curve of a combustion experiment is shown in Fig. 4.

4.1. Procedure to Determine the Adiabatic Temperature Rise

Compared to the adiabatic calorimeter, an additional temperature correction term, ΔT_{ex}, describing the heat exchange with the surroundings

is added in order to determine the adiabatic temperature rise in an isoperibolic calorimeter as exposed by

$$\Delta T_{\mathrm{ad}} = T_{\mathrm{mf}} - T_{\mathrm{mi}} - \Delta T_{\mathrm{ex}} \tag{5}$$

The heat balance in Eq. (3) divided by $m_{\mathrm{cal}} c_{\mathrm{p,cal}}$ is used to determine the adiabatic temperature difference, ΔT_{ad}.

$$\frac{dT_{\mathrm{cal}}(t)}{dt} = u(t) + u_{\mathrm{stir}} + k(T_0 - T_{\mathrm{cal}}(t)) \tag{6}$$

where

$u(t)$ is the temperature rate due to heat production (combustion, enthalpy differences, and ignition),

u_{stir} is the temperature rate due to heat production (stirrer), and

k is the cooling constant of the calorimeter $(=\kappa/(m_{\mathrm{cal}} c_{\mathrm{p.cal}}))$

On the left-hand side of Eq. (6), T_{cal} means the *volume averaged temperature* of the calorimeter. However, as has been mentioned before, the heat transfer depends on the temperature difference between the water jacket temperature T_0 and the surface averaged temperature. For an ideal calorimeter the volume averaged temperature equals the *surface averaged temperature*. In reality both temperatures may slightly differ. For the determination of ΔT_{ad} the temperature is measured at the location of the sensors as representative of both averaged temperatures. Due to technical constraints, it is only possible to minimize temperature gradients, but they will still remain at a certain level. The uncertainty arising from this fact is a question of carrying out electrical calibration and combustion identical in such a way that the temperature fields of both processes are equal as a function of time.

The value of the cooling constant, k, in Eq. (6) governs the heat transfer between the calorimeter and its surroundings. k is a constant of the calorimeter. Applying Eq. (6) to the initial and final periods of the experimental temperature–time curve only allows calculation of the k-value. Under these restrictions, $u(t)$ is zero and u_{stir}, the temperature rate due to heat production by the stirrer, is constant. Moreover, T_0, the temperature in the water jacket, is constant. Therefore, T_∞, the temperature of the calorimeter bath at infinite time, may be defined by

$$\lim_{t \to \infty} T : 0 = u_{\mathrm{stir}} + k(T_0 - T_\infty) \tag{7}$$

Thus, the temperature during the initial and final period for the combustion or calibration experiment follows the relation,

$$\frac{dT_{\mathrm{cal}}}{dt} = k(T_\infty - T_{\mathrm{cal}}(t)) \tag{8}$$

Using Eq. (8) an exponential analytical expression for the initial and final periods may be obtained. For the initial period (subscript i), it follows that

$$T_{\mathrm{i}}(t) = T_\infty - (T_\infty - T_{\mathrm{mi}})\exp(-k(t - t_{\mathrm{mi}})) \tag{9}$$

where

T_{mi} is the temperature at the beginning of the main period (end of initial period) and

t_{mi} is the time at the beginning of the main period.

In a new analytical approach, the constants k and T_∞ are determined by a simultaneous regression of the temperature–time data in the initial and final periods. This analytical fitting procedure of the temperatures $T_{\mathrm{i}}(t)$ and $T_{\mathrm{f}}(t)$ is applied for the first time. The temperature correction term, ΔT_{ex}, for the main period can now be calculated assuming constant values for k and T_0 during the whole experiment:

$$\Delta T_{\mathrm{ex}} = k \int_{t_{\mathrm{mi}}}^{t_{\mathrm{mf}}} (T_\infty - T_{\mathrm{cal}}(t))dt \tag{10}$$

Thus, all information is available to determine the adiabatic temperature rise. Equations (9) and (10) are derived under the following assumptions:

(a) The heat transfer due to convection or radiation is small.

(b) The temperature, T_0, and the quantities k and u are constants.

(c) The measured temperatures, $T_{\mathrm{i}}(t)$, $T_{\mathrm{cal}}(t)$, and $T_{\mathrm{f}}(t)$, are *assumed* to be the averaged temperatures of the calorimeter. No distinction is made between surface or volume averaged temperatures.

The uncertainties arising from these assumptions will be discussed below. The measured temperature–time curve is analyzed through Eqs. (9) and (10) using the *Simpson* rule for numerical integration during the main period, i.e., the combustion period. ΔT_{ad} is given by Eq. (5).

4.2. Temperature Measurement

The temperature measurements must be sensitive and have fast response to temperature changes. In the past [2,3,9] resistance thermometers were often used in isoperibolic combustion calorimetry following the

Rossini principle. However, due to the sluggish response of the platinum resistance thermometer, they can be used reasonably in the initial and final periods only. In this study, the fast temperature rise during the main period is measured with a fast response thermistor sensor. In our arrangement, the thermistor is calibrated against the traceable Pt25 resistance thermometer *in situ* at each experimental run using balanced Pt25 data of the initial and final periods.

Before the experimental run starts, the calorimeter is cooled to 23°C and the temperature in the water jacket is set to 26.8°C. After an equilibration interval of about 1 h, the initial period starts and lasts for approximately 30 min. During the initial period, no gas flows through the calorimeter. When the calorimeter temperature has reached 23.5°C, the gas flow and ignition start simultaneously. Combustion continues for about 25 min. The start time of the main period t_{mi} is the time of ignition. In an electrical calibration this time corresponds to the time of switching the electrical heater on. Immediately after extinction of the flame during the main period, the gas flow through the calorimeter is stopped and all valves are closed.

5. CALCULATION OF THE CALORIFIC VALUE

After the description of the experimental set-up and operation procedures, the formal method for evaluation of the superior calorific value, H_s, shall be described in detail. As already mentioned, the principle of the gas calorimeter is based on the heat comparator method.

This method is expressed by the ratio of the chemical energy released during the combustion of the respective fuel gas to the electrical energy released during a calibration run;

$$\frac{E_{comb}}{E_{elec}} = \frac{C_{cal,comb}\Delta T_{ad,comb}}{C_{cal,elec}\Delta T_{ad,elec}} \tag{11}$$

The combustion energy, E_{comb}, may be expressed by the product of the mass of the burnt gas, m_{gas}, and the superior calorific value, H_s, (corrected by the energy correction term K). Inserting this information into Eq. (11) leads to the following equation:

$$\frac{m_{gas}H_s - K}{E_{elec}} = \frac{C_{cal,comb}\Delta T_{ad,comb}}{C_{cal,elec}\Delta T_{ad,elec}} \tag{12}$$

This equation may directly be solved for the superior calorific value, H_s:

$$H_s = \frac{E_{elec}C_{cal,comb}\Delta T_{ad,comb}}{m_{gas}C_{cal,elec}\Delta T_{ad,elec}} + \frac{K}{m_{gas}} \tag{13}$$

The first assumption, prerequisite, of the heat comparator model (see Eqs. (11) or (12)) is that the calorimeter may be operated as a comparator, i.e., the amount of heat released in the combustion experiment is about the same as the heat released during electrical calibration. This assumption requires that the numerator, $C_{\mathrm{cal,comb}}\Delta T_{\mathrm{ad,comb}}$, and the denominator, $C_{\mathrm{cal,elec}}\Delta T_{\mathrm{ad,elec}}$, on the right-hand side of Eq. (12) are about equal. The second assumption is that the heat capacities of both processes are nearly the same. Therefore, it is necessary that the calorimeter is not changed between a calibration and a combustion run, and the calorimeter is operated at the same conditions (same absolute temperatures, temperature rises, stirrer speeds, etc.). Then the only systematic difference other than the energy correction, K, is the condensation of water vapor inside the burner–heat exchanger system. This water formed by the combustion process leads to a significant additional heat capacity as a function of time during the main period. For these reasons the most important requirement is the equality of the adiabatic temperature rises ΔT_{ad} of the combustion and respective calibration experiment.

As a result, the right-hand side of Eq. (12) may be expressed as a dimensionless factor, F, which can be divided into a factor F_C (contribution of the heat capacities) and a factor $F_{\Delta T_{\mathrm{ad}}}$ (contribution of the adiabatic temperature rises);

$$F = \frac{C_{\mathrm{cal,comb}}\Delta T_{\mathrm{ad,comb}}}{C_{\mathrm{cal,elec}}\Delta T_{\mathrm{ad,elec}}} = F_C F_{\Delta T_{\mathrm{ad}}} \tag{14}$$

whereas the experiments have to be carried out in the same operating point indicated by

$$F_{\Delta T_{\mathrm{ad}}} = 1 \tag{15}$$

Equations (14) and (15) show clearly the two influences on the "identity" of the combustion and calibration processes. Due to the experimental temperature–time curves, $F_{\Delta T_{\mathrm{ad}}}$ can be matched equal to 1. The value of $C_{\mathrm{cal,elec}}$ is determined by the electrical calibration run. However, the value of $C_{\mathrm{cal,comb}}$ implemented in the factor F_{C} cannot be determined experimentally. To overcome this problem, at least two conditions must be fulfilled: first, the calorimeter system must not change between the combustion and calibration experiment (the amount of water must be constant, the mechanical parts must be the same and in the same position). Second, the sum of the heat capacities of the calorimeter components should not change significantly with temperature and time under the experimental conditions. This has been proven by the calculation of the respective temperature-induced change of c_p of the main components, water, steel, and glass. Therefore, the second condition is fulfilled. The first

condition is also fulfilled, because the respective combustion and calibration run is operated at as similar conditions as possible directly successive in time (usually, both experiments in 2 days). This means that F_C is very close to 1 (e.g., 1.0004) as a matter of principle.

Using the dimensionless factor F, Eq. (13) can be expressed as

$$H_s = \frac{E_{elec} F}{m_{gas}} + \frac{K}{m_{gas}} \tag{16}$$

At this point important additional information must be pointed out with respect to the ratio F. Due to the progressive condensation of water with mass m_{cond,H_2O} during combustion inside the burner glass vessel, the heat capacity of the calorimeter increases during the combustion experiment. This change is included in $C_{cal,comb,f}$, the heat capacity of the calorimeter at the end of the main period or in the final period. During the initial period or at the beginning of the main period, $C_{cal,comb,i} = C_{cal,elec}$. Therefore, in the calculation of the heat of combustion, $C_{cal,comb}\Delta T_{ad,comb}$, in Eq. (12), a time averaged value for the heat capacity, $C_{cal,comb}$, matches the time-dependent condensation of water during the combustion process;

$$C_{cal,comb} \approx C_{cal,elec} + w m_{cond,H_2O} c_{p,H_2O} \tag{17}$$

The factor w has to be calculated for each combustion run and can be found in a range between 0.5 and 0.8.

The heat capacity of the calorimeter is determined by the electrical calibration experiment;

$$C_{cal,elec} = \frac{E_{elec}}{\Delta T_{ad,elec}} \tag{18}$$

The electrical energy is determined as the sum of i time intervals Δt_i (2 s);

$$E_{elec} = \sum_i \frac{U_{heat,i} U_{ref,i}}{R_{ref,i}} \Delta t_i \tag{19}$$

where

U_{heat} is the voltage drop at the electrical heater and

U_{ref} is the voltage drop at the reference resistance R_{ref}.

The adiabatic temperature rises ΔT_{ad} in Eq. (14) are determined as described above (see Eq. (5)).

The correction term, K, for the determination of the calorific value in Eq. (16) accounts for the following contributions:

$$K = E_w + E_g - E_i \tag{20}$$

where

E_i is the ignition energy,

E_w is the energy term due to water vapor leaving the calorimeter, and

E_g is the energy due to temperature differences of the gases between in- and out-flow of the calorimeter.

So far, the procedure to evaluate the calorific value, H_s, has been described. However, during the development of the reference calorimeter, it became evident that additional influences play an important role in determining the absolute value and the uncertainty budget of the calorific value. To handle these contributions in an analytical form is extremely difficult. Therefore, separate investigations helped to quantify the following uncertainty contributions:

- uncertainties arising from the type of mathematical model for calculating ΔT_{ad},
- variation of the time interval length Δt_{mf} in these calculation procedures,
- position of the temperature sensor in the calorimeter, and
- position of the electrical heat release in the calibration experiment.

In addition to the classical error propagation law, the corresponding uncertainties have to be taken into account as uncertainty increments. Besides experimental variations, a computer simulation of the calorimeter gives additional insight into the behavior of the system, especially for the temperature and flow field.

6. SIMULATION OF FLOW AND TEMPERATURE FIELD

The operation of the calorimeter and the evaluation of results, in particular, depend on some conditions to be fulfilled with a high degree of accuracy. As indicated above, the heat balance on the inner calorimeter vessel is governed by Eq. (7). This equation relates the time derivative of the volume averaged calorimeter temperature to the heat transfer between the inner and outer calorimeter vessels, the exchange of enthalpy by adding and withdrawing gases, and the heat production by combustion and dissipation of the kinetic energy introduced by the stirrer. The heat transfer between the calorimeter and water jacket is calculated from a global heat transfer coefficient multiplied by the difference of the jacket temperature and the surface averaged calorimeter temperature.

This approach implies that the temperature distribution is homogeneous inside the calorimeter and that the heat transfer coefficient is constant during the complete process. Both the requirements must hold for combustion as well as for calibration cycles. Additionally, the thermal properties of both types of cycles must match closely.

In order to verify whether these conditions are met with sufficient accuracy, numerical simulations of the flow and of thermal processes were performed. The simulations provide detailed information that is difficult to obtain experimentally. This, however, requires the physical process to be modeled as close to reality as possible.

The numerical model comprises the inner and outer calorimeter vessels. At the surface of the outer vessel, the temperature was assumed to be constant and equal to the temperature of the water jacket. The numerical results presented below were calculated assuming a temperature, $T_0 = 300\,\mathrm{K}$. The actual geometry and its numerical counterpart are identical except for a few differences.

(a) In order to avoid an exceedingly high number of computational nodes and unduly high-computational times, the motion of the stirrer was not modeled. Instead, the problem was simplified by replacing the stirrers inside the stirrer channel with interfaces that allow for specifying the pressure jump and the swirl generated by the propellers (fan interfaces are an option of the numerical solver FLUENT employed here). The fan boundary conditions, pressure jump and swirl, were measured prior to the simulation and estimated from the shape of the propeller.

(b) Methane combustion was treated assuming a two-step reaction mechanism:

$$\mathrm{CH_4} + 1.5\mathrm{O_2} \rightarrow \mathrm{CO} + 2\mathrm{H_2O}$$

$$\mathrm{CO} + 0.5\mathrm{O_2} \rightarrow \mathrm{CO_2}$$

(c) The only physical effect that was impossible to be taken into account was condensation of the water vapor generated by the above chemical reactions. Since water leaves the numerical model in the gaseous form, the heat of condensation is not released. Thus, heat transfer from the flue gases to the calorimeter water is less than in reality.

Since the geometry of the calorimeter is fairly complex, about 4 million computational nodes were required to properly resolve the computational domain. The simulations have to account for the heating of the reservoir and, thus, had to be run in the unsteady mode. Due to the large computational grid and the complicated physics, each second simulated requires 6 h of physical time when the job is run on four processors of a V880 Fujitsu Siemens computer server. The simulation provides detailed

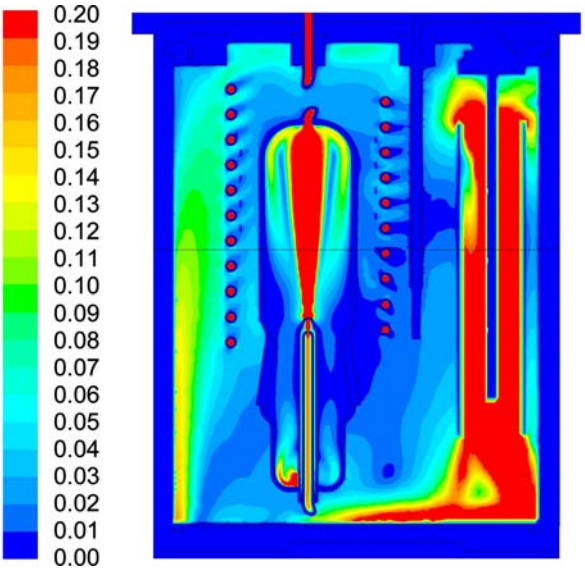

Fig. 5. Velocity distribution (in $m \cdot s^{-1}$) in the symmetry plane of the calorimeter during combustion. All velocities above $0.20\,m \cdot s^{-1}$ are indicated in red.

information on the velocity, temperature, and concentration fields. Additionally, heat fluxes by radiation and convection as well as similar quantities can be evaluated.

Figure 5 shows an example of a contour plot of the velocity distribution in the vertical symmetry plane of the calorimeter. The swirl generated by the stirrers was supposed to be removed by flow straighteners introduced into the stirrer channel. The simulated image shows that the water emanating from the channel exit generates a jet-like flow. The jet is deflected upwards by the wall opposite to the stirrer channel and splits into two main streams. One of them passes along the cooling coil and the burning chamber in the vertical direction. The second one impinges on both devices and receives energy from the heated surfaces. Thus, elevated temperatures prevail in the space between the heater and stirrer channel (cf. Fig. 6). The velocity, however is fairly low there, since this region is located in the wake of the burning chamber.

Figure 6 shows the temperature distribution in the vertical symmetry plane of the calorimeter during combustion. The simulation reveals that the temperature distribution in the calorimeter water varies by $\pm 0.1\,K$. The water jacket temperature was set to $T_0 = 300\,K$. For the instant

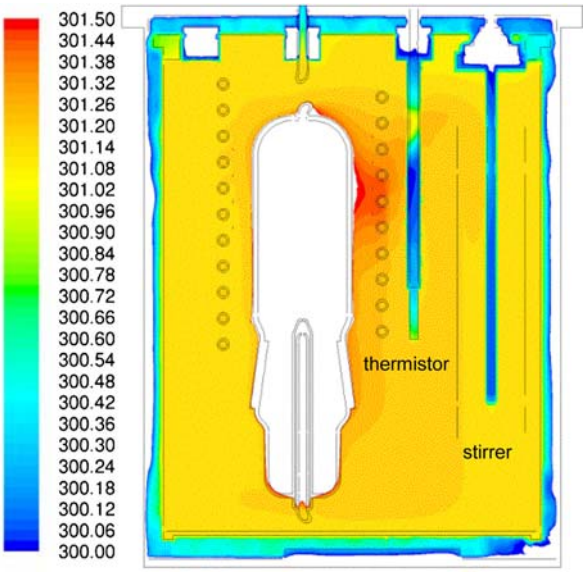

Fig. 6. Temperature distribution (in K) in the symmetry plane of the calorimeter during combustion. Areas with temperatures above 301.5 K and below 300 K are blank.

considered in Fig. 6, the following temperatures are calculated from the numerical data:

the volume average of temperature is $\bar{T}_{\mathrm{cal,volum}} = 301.066\,\mathrm{K}$,

the surface averaged temperature is $\bar{T}_{\mathrm{cal,surfa}} = 301.155\,\mathrm{K}$,

the temperature of the Pt25 was found to be $T_{\mathrm{Pt25}} = 301.163\,\mathrm{K}$, while

the thermistor was at a fairly low temperature $T_{\mathrm{therm}} = 300.509\,\mathrm{K}$.

The combustion process started at an initial temperature $T_{\mathrm{mi}} = 300\,\mathrm{K}$. The thermistor position is in the vertical symmetry plane between the burner and the stirrer. Therefore, it is located in the low velocity area between the stirrer channel and burning chamber and heats up slower than, for instance, the Pt25, although it has a shorter response time to temperature. The Pt25, however, is positioned in front of the thermistor at about 2/3 of its distance to the wall of the calorimeter vessel. Therefore, it follows closer to the average calorimeter temperature as it is directly exposed to the flow.

The temperature distribution in the calorimeter with electrical heating in Fig. 7 results in a simulation starting at the same identical initial

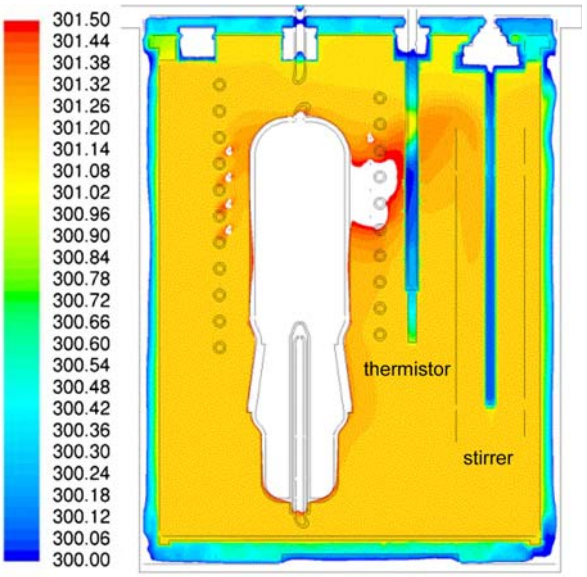

Fig. 7. Temperature distribution (in K) in the symmetry plane of the calorimeter during electrical heating. Areas with temperatures above 301.5 K and below 300 K are blank.

temperature distribution as in the combustion simulation. The same heat input was now introduced by an electrical heater with a heating coil placed in the upper part of the calorimeter between the combustion chamber and the heat exchanger. As the velocities in the wake of the combustion chamber are small, the high heat input into this region by the electrical heater cannot sufficiently be distributed in the calorimeter by convection; therefore, locally high temperatures occur. The following numerical results are obtained.

The temperatures at the Pt25 and the thermistor locations are the same as before, whereas the averaged temperatures differ slightly:

the volume average of temperature is $\bar{T}_{\mathrm{cal,volum}} = 301.086\,\mathrm{K}$,

the surface averaged temperature is $\bar{T}_{\mathrm{cal,surfa}} = 301.181\,\mathrm{K}$,

As indicated above, the outer surface temperature of the calorimeter vessel governs the heat transfer between the calorimeter and water jacket. When employing Eq. (7) for the evaluation of the calorific value from experiments, it is desirable for the surface temperature to match the volume-averaged temperature of the calorimeter as closely as possible.

When employing the energy comparator method to analyze the calorimeter results, the combustion and electrical calibration process need to be very closely matched. From the numerical results the surface averaged temperature is about 0.1 K higher than the volume averaged value. The numerical results for the electrical calibration process are approximately 0.02 K higher than for the combustion process. This results from a numerical simulation which used a value of 2 W for the combined convective and radiative heat flux from the inner to the outer calorimeter vessel. Meanwhile, this value for the actual calorimeter setup is reduced to approximately 1 W.

Due to the results of the simulation, the conventional calorimetric practice to measure the temperature at one certain position inside the calorimeter is questionable. Is there any difference for the calorific value, if another position for the temperature sensor is chosen? What happens if instead of a position inside the calorimeter can (i.e., a temperature in the volume) the temperature is measured on the surface of the calorimeter can? In addition, it can be seen from the simulation that the position of the heat source (i.e., burner or electrical heater) result in different temperature fields. For this reason there is also the question whether different positions of the electrical heat release lead to different results for the calorific value? These questions can be answered only by experiment. Corresponding investigations were carried out to vary the location of the temperature sensor and also the heat release. Through the use of such experiments, uncertainty contributions can be determined which are due to the experimental calorimetric procedure. To investigate the effects of heater and temperature sensor positions, combustion runs and corresponding electrical calibration runs have been carried out with the prototype calorimeter. Due to the fact that the repeatability of the results of this prototype has not reached the final intended state, at this stage the results can be understood as an estimate only.

7. PROCEDURE-DEPENDENT UNCERTAINTIES

The determination of the calorific value is influenced by additional uncertainties which to the best of our knowledge have not been considered in the past. However, they have some influence on the correct determination of H_s:

7.1. Uncertainty due to the Analytical Model

The values of the adiabatic temperature rise ΔT_{ad} depend on the choice of the analytical model. In the past, modified versions of the

Regnault–Pfaundler method or the comparison of equal areas called "the Dickinson method" [14] have been typically applied. In this work the adiabatic temperature rise is determined analytically by fitting the temperatures of the initial ($T_i(t)$) and final period ($T_f(t)$) simultaneously to an exponential function due to the solution of the partial differential equation (Eq. (8)). The conventional approach of using a linear regression for the initial and final periods is in contrast to the mathematical solution and is not considered further.

The temperature correction term, ΔT_{ex}, describing the heat exchange with the surroundings is determined by a numerical integration of the main period. The numerical integration can be performed using the *Trapezoidal* rule or the *Simpson* rule. The latter is known to be 100 times more precise than the *Trapezoidal* rule. We have applied a set of 12 different analytical models for the evaluation of ΔT_{ad}. Table II summarizes the 12 applied methods.

Method number 10 applied by the Office for Gas and Electricity Markets (OFGEM, UK) uses a linear regression of the data of the initial and final periods for the determination of k. Then the time axis is transformed into an exponential scale and T_∞ is determined by extrapolation.

When using the physically reasonable methods 1 and 7 (e.g., simultaneous exponential fit of the initial and final periods, integration using the *Simpson* rule), the ratios of the calculated adiabatic temperature rises for combustion and electrical calibration differ by 1.4×10^{-4} at a maximum. At this time it cannot be decided whether method 1 or 7 should be preferred. This will be a task of subsequent investigations. From this value (considered as a rectangle distribution), the corresponding uncertainty δF_{model} was calculated and is displayed in Table III.

7.2. Uncertainty due to Variation of Time Interval Length in Data Analysis

The variation of the arbitrarily chosen interval length of the main period (Δt_{mf}) is implemented by N calculations of ΔT_{ad} (combustion as well as calibration experiment) varying Δt_{mf} in a stepwise addition of 100 s around a physically reasonable value of Δt_{mf}. In Eq. (21), combinations of ratios $\Delta T_{ad,comb}/\Delta T_{ad,elec}$—adiabatic temperature rises of combustion and calibration—are used by varying the interval length (time Δt_{mf}) of the main period from $i = 1 \ldots N$ ($N = 15$):

Table II. Comparison of Applied Analytical Models for the Determination of ΔT_{ad}

	Method	Fit of T-data: k, T_∞ initial/finalperiod	Determination of ΔT_{ex} (integration method)
1	equal areas (*Dickinson*)	simultaneous exponential: $k_i, k_f, T_{\infty,f}$	equal areas
2	equal areas (*Dickinson*)	separate exponential: k_{mean}, $T_{\infty,mean}$ (arithm. mean)	equal areas
3	equal areas (*Dickinson*)	separate exponential: $k(t,T), T_\infty(t,T)$	equal areas
4	*Regnault*/*Pfaundler*	simultaneous exponential: $k_i, k_f, T_{\infty,f}$	trapezoidal
5	*Regnault*/*Pfaundler*	separate exponential: $k_{mean}, T_{\infty,mean}$ (arithm. mean)	trapezoidal
6	*Regnault*/*Pfaundler*	separate exponential: $k(t,T), T_\infty(t,T)$	trapezoidal
7	*Regnault*/*Pfaundler*	simultaneous exponential: $k_i, k_f, T_{\infty,i}, T_{\infty,f}$	*Simpson*-rule
8	*Regnault*/*Pfaundler*	separate exponential: $k_{mean}, T_{\infty,mean}$ (arithm. mean)	*Simpson*-rule
9	*Regnault*/*Pfaundler*	separate exponential: $k(t,T), T_\infty(t,T)$	*Simpson*-rule
10	*OFGEM*	k: linear regression, T_∞: extrapolation	trapezoidal
11	*Regnault*/*Pfaundler*	simultaneous linear: $k_i, k_f, T_{\infty,i}, T_{\infty,f}$	trapezoidal
12	*Regnault*/*Pfaundler*	simultaneous linear: $k_i, k_f, T_{\infty,i}, T_{\infty,f}$ two data points per period	trapezoidal

Table III. Procedure-Dependent Uncertainty Contributions

Uncertainty contributions to HS	
	$U(k=1)$
δF_{model}	$2.2\,kJ \cdot kg^{-1}$
$\delta F_{\Delta_{tmf}}$	$2.9\,kJ \cdot kg^{-1}$
$\delta F_{sensor\ position}$	$1.6\,kJ \cdot kg^{-1}$
$\delta F_{heater\ position}$	$1.6\,kJ \cdot kg^{-1}$

$$F_{\Delta T_{\mathrm{ad}}} = \frac{1}{N}(\Delta T_{\mathrm{ad,comb\,1}}/\Delta T_{\mathrm{ad,elec\,1}} + \cdots + \Delta T_{\mathrm{ad,comb\,N}}/\Delta T_{\mathrm{ad,elec\,N}}) \quad (21)$$

The values of the ratio differ by 1.8×10^{-4} at a maximum. Considering for this value a rectangle distribution, an additional uncertainty $\delta F_{\Delta \mathrm{tmf}}$ was calculated.

7.3. Uncertainty due to the Location of the Temperature Sensor

Varying the location of the temperature sensor may directly demonstrate temperature inhomogeneities as has been shown by the computer simulation. Here, the temperatures inside the calorimeter and the temperature on the surface of the calorimeter were measured simultaneously with a resistance thermometer and with a calibrated copper wire, respectively. The ratios for the adiabatic temperature rise differ by 1×10^{-4}. From this value considering a rectangle distribution, the uncertainty $\delta F_{\mathrm{sensor\,position}}$ was calculated (Table III).

7.4. Uncertainty due to the Location of Heat Release

A key factor of the application of the heat comparator model is the equality of the combustion and calibration experiment and the corresponding heat capacities. Experiments were carried out by splitting the heat release (100% or 90% were released by the original heater in combination with 0% or 10% released by an additional heater located in the cooling finger position). These experiments led only to a difference of 1×10^{-4} for the ratios of the adiabatic temperature rise. Again, this difference was considered as a rectangle distribution to calculate the uncertainty $\delta F_{\mathrm{heater\,position}}$ (Table III).

Table III shows the investigated absolute uncertainty contributions related to the calorific value of methane ($55515.18\,\mathrm{kJ \cdot kg^{-1}}$ [4]) according to the GUM guide [15]. The four considered absolute uncertainties together result in a relative uncertainty of 0.015% ($k = 2$, i.e. at a confidence level of 95%). This is only a part of the total uncertainty budget. However, it shows, that these contributions play a significant role and cannot be neglected.

8. CONCLUSION AND OUTLOOK

A new state-of-the-art reference gas combustion calorimeter was setup and a corresponding computer simulation of the temperature and flow fields was carried out. From the computer simulation it has been shown

that the temperature field shows inhomogeneities, which were not taken into account in previous investigations. For this reason, experiments varying the temperature sensor position and the electrical heater position were carried out to estimate related uncertainties for the calorific value. In addition, different mathematical procedures for the data analysis of the temperature–time curves have been investigated. It has been shown that a procedure-dependent uncertainty results due to the type of mathematical model used. Also, the change of the length of the main period yields an additional uncertainty. Considering the calorific value of methane, the mentioned uncertainties may contribute as much as 0.015% to the uncertainty of the calorific value. Finally, this investigation shows that the considered uncertainty contributions, which have not been considered in the past, may contribute an important amount to the targeted overall uncertainty of 0.05% for the calorific value. In addition, all the other uncertainty contributions related to the experimental quantities have to be taken into account. These will be calculated when a sound basis of experimental runs has been carried out.

ACKNOWLEDGMENTS

The authors gratefully acknowledge both financial as well as scientific support from Enagas, Spain; E.ON Ruhrgas AG, Germany; Gaz de France, France; Laboratoire National D'Essais, France; Physikalisch-Technische Bundesanstalt, Germany; and Snam Rete Gas, Italy.

REFERENCES

1. P. Ulbig and S. Kimpton, in *Proc. Advanticas Gas Quality Conf.*, Loughborough, United Kingdom (2002).
2. F. D. Rossini, *J. Res. Nat. Bur. Stand. (U.S.)* **6**:1 (1931); *J. Res. Nat. Bur. Stand. (U.S.)* **6**:37 (1931); *J. Res. Nat. Bur. Stand. (U.S.)* **7**:329 (1931).
3. D. A. Pittam and G. Pilcher, *J. Chem. Soc., Faraday Trans. I* **68**:2224 (1972).
4. *ISO 6976*, "Natural Gas – Calculation of Calorific Values, Density, Relative Density and Wobbe Index from Composition" (International Organization for Standardization, Geneva, 1995).
5. *ISO 15971*, "Natural gas – Measurement of Properties, Combustion Properties, Calorific Value and Wobbe Index" (International Organization for Standardization, Geneva, 2007).
6. *ASTM D 4891-89*, "Standard Test Method for Heating Value of Gases in Natural Gas Range by Stoichiometric Combustion" (1989).
7. M. Jaeschke, P. Schley, and R. Janssen-van Rosmalen,*Int. J. Thermophys.* **23**:1013 (2002).
8. P. Schley, M. Jaeschke, and K. Altfeld, presented at the *22nd World Gas Conf.*, Tokyo, Japan (2003).
9. P. Wenz, P. Ulbig, and S. Sarge, *J. Therm. Anal. Calorim.* **71**:137 (2003).

10. P. Ulbig, A. Benito, P. L. Cremonesi, J.-R. Filtz, R. Forster, F. Haloua, B. Hay, M. Jaeschke, S. Loubat, S. Sarge, and P. Wenz, in *11th Conf. Flow Measurement (Flomeko)*, Groningen, The Netherlands (2003).
11. A. Dale, C. Lythall, J. Aucott, and C. Sayer, *Thermochim. Acta* **382**:47 (2002).
12. P. Cowan and A. E. Humphreys, in *Proc. Congress of* "*Gas Quality – Specifications and Chemical Properties of Natural Gas*," G. J. van Rossum, ed. (Elsevier Science Pubs. B.V., Groningen, Netherlands, 1986), pp. 169–179.
13. S. Sunner, in *Combustion Calorimetry, Experimental Chemical Thermodynamics*, Vol. 1, S. Sunner and M. Mansson, eds. (Pergamon Press, New York, 1981), pp. 13–34.
14. W. A. Roth and F. Becker, *Kalorimetrische Methoden* (F. Vieweg & Sohn, Braunschweig, 1956).
15. *Guide to the Expression of Uncertainty in Measurement*, 1st Ed. (1993), corrected and reprinted (1995) (International Organization for Standardization, Geneva).